Cancer Research

Wnt5a Drives an Invasive Phenotype in Human Glioblastoma Stem-like Cells

Elena Binda[1], Alberto Visioli[2], Fabrizio Giani[3], Nadia Trivieri[4], Orazio Palumbo[5], Silvia Restelli[2], Fabio Dezi[1], Tommaso Mazza[4], Caterina Fusilli[4], Federico Legnani[6], Massimo Carella[5], Francesco Di Meco[6,7], Rohit Duggal[8], and Angelo L. Vescovi[1,3,4,9]

Abstract

Brain invasion by glioblastoma determines prognosis, recurrence, and lethality in patients, but no master factor coordinating the invasive properties of glioblastoma has been identified. Here we report evidence favoring such a role for the noncanonical WNT family member Wnt5a. We found the most invasive gliomas to be characterized by Wnt5a overexpression, which correlated with poor prognosis and also discriminated infiltrating mesenchymal glioblastoma from poorly motile proneural and classical glioblastoma. Indeed, Wnt5a overexpression associated with tumor-promoting stem-like characteristics (TPC) in defining the character of highly infiltrating mesenchymal glioblastoma cells (Wnt5a^{High}). Inhibiting Wnt5a in mesenchymal glioblastoma TPC suppressed their infiltrating capability. Conversely, enforcing high levels of Wnt5a activated an infiltrative, mesenchymal-like program in classical glioblastoma TPC and Wnt5a^{Low} mesenchymal TPC. In intracranial mouse xenograft models of glioblastoma, inhibiting Wnt5a activity blocked brain invasion and increased host survival. Overall, our results highlight Wnt5a as a master regulator of brain invasion, specifically TPC, and they provide a therapeutic rationale to target it in patients with glioblastoma. *Cancer Res; 77(4); 996–1007. ©2016 AACR.*

Introduction

To date, human grade IV gliomas (glioblastomas; hGBM) are incurable tumors. Average survival barely exceeds 16 months even with the best and most aggressive therapies (1, 2). In combination with uncontrolled growth, the hGBM cells rapidly migrate and spread throughout the brain tissue, thereby eluding surgical ablation and radiotherapy. This deadly combination represents a nearly insurmountable obstacle for the development of effective therapies for high-grade gliomas (3, 4). Understanding of the key mechanisms that are responsible for the inherent ability of hGBM cells to migrate and invade the brain parenchyma is vital for the identification of new, more effective therapies.

Significant progress has been made in unraveling the many signaling moieties that elicit invasiveness in hGBM cells. Numerous intertwined pathways, such as TGFβ, Sonic Hedgehog, PI3K/Akt signaling, and epigenetic regulators enhance cleavage of the extracellular matrix in the brain and foster glioma cell invasion (5). Many of these pathways impinge on common effectors, such as protease activation or degradation of β-catenin (6, 7). The Notch and Wnt/β-catenin signaling pathways can also activate an epithelial-to-mesenchymal–like program in malignant gliomas, thereby modulating the motility of hGBM cells and their invasiveness (8).

These findings notwithstanding, the perspective existence, identity, and functions of key master regulatory factors that, *per se*, can globally drive the network of signaling pathways bestowing the invasive phenotype upon hGBM cells remain undetermined. The pleiotropic functions carried out by Wnt proteins in neurogenesis and stem cell proliferation and differentiation make members of this family good candidates for this role. Deregulation of the Wnt signaling pathway is often associated with the induction and progression of cancer in several tissues, including the CNS (ref. 9; reviewed in refs. 10, 11). Various members of the Wnt family can activate β-catenin–dependent intracellular signaling (12). This occurs through the binding of the canonical Wnts, such as Wnt1, Wnt3a, or Wnt7a, to specific surface receptor complexes, which induces the stabilization of cytoplasmic β-catenin and promotes its nuclear entry. Once in the nucleus, β-catenin stimulates the transcription of target genes, thus promoting predominantly glioma cell proliferation via TCF/LEF family of transcription factors (13). If the Wnt/β-catenin pathway is blocked, an antineoplastic response is normally observed (14). Most notably, noncanonical Wnts such as Wnt2, Wnt4, Wnt5a, Wnt6, and Wnt11 modulate predominantly cell movement and polarity through the

[1]IRCSS Casa Sollievo della Sofferenza, ISBReMIT- Institute for Stem Cell Biology, Regenerative Medicine and Innovative Therapies, Italy. [2]StemGen SpA, Milan, Italy. [3]Dept. of Biotechnology and Biosciences, University of Milan Bicocca, Milan, Italy. [4]IRCSS Casa Sollievo della Sofferenza, c/o Instituto Mendel, Rome, Italy. [5]Medical Genetics Unit, IRCSS Casa Sollievo della Sofferenza, Opera di San Pio da Pietrelcina, Italy. [6]National Neurological Institute "C. Besta," Milan, Italy. [7]Department of Neurosurgery, John Hopkins University, Baltimore, Maryland. [8]Stem Cell Research Unit, Sorrento Therapeutics Inc., San Diego, California. [9]Hyperstem SA, Lugano, Switzerland.

Note: Supplementary data for this article are available at Cancer Research Online (http://cancerres.aacrjournals.org/).

Corresponding Authors: Angelo L. Vescovi, IRCSS Casa Sollievo della Sofferenza, Opera di San Pio da Pietrelcina, viale dei Cappuccini, S. Giovanni Rotondo, Foggia 71013, Italy. Phone: 39-334-5845694; Fax: 39-0882-416568; E-mail: vescovia@gmail.com; and Elena Binda, IRCSS Casa Sollievo della Sofferenza, ISBReMIT, viale dei Cappuccini 1, 71013 S. Giovanni Rotondo, Foggia, Italy. Phone: 39-344-2352249; E-mail: e.binda@css-mendel.it

doi: 10.1158/0008-5472.CAN-16-1693

©2016 American Association for Cancer Research.

AACR

activation of β-catenin–independent pathways (15). Of importance, it appears that canonical and noncanonical Wnts, particularly Wnt3a and Wnt5a (16), may be somewhat intertwined and can operate to antagonize one another (17).

Deregulation/upregulation of Wnt5a has been linked to cancer invasion and metastasis in some solid tumors (18–22), yet little is known about its actual pathophysiological role in hGBMs. It has been shown that Wnt5a is overexpressed in high-grade gliomas, but the role for Wnt5a in regulating proliferation and migration in gliomas has only been demonstrated, in a few cell lines, *in vitro* (23–27). Here, we explore whether Wnt5a can function as a master regulator of the invasive capacity of hGBMs. We demonstrate that exacerbated Wnt5a expression is associated with, and single handedly responsible for, the manifestation of an exacerbated functional and molecular invasive phenotype in glioma cells, whereas its inhibition produces the opposite effects. Notably, this phenomenon occurs in tumor-promoting stem-like cells (TPC; refs. 28–30), aka the cancer stem cell population. The effects that we observed upon inhibition of Wnt5a in an intracranial xenograft hGBM model suggest that this approach may have notable, putative therapeutic implications for the cure of these tumors.

Materials and Methods

Primary cell culture and culture propagation

hGBM, anaplastic, and low-grade gliomas tissue samples were obtained in accordance with research ethics board approval from the National Neurological Institute "C. Besta" (Prot. 02) and classified according to the World Health Organization guidelines. hGBM patient–derived TPCs were isolated as previously described (28, 31). Primary (acutely dissociated cells) or established TPCs were plated in NeuroCult NS-A medium (Stemcell Technologies), containing 20 ng/mL of EGF (PeproTech) and 10 ng/mL of FGF2 (PeproTech; ref. 28). As reference, human neural stem cell (hNSC; ref. 32) and the human glioma cell line U87MG were employed. Cell line authenticity was last tested in January 2016 using CNV profiling.

Immunofluorescence and immunohistochemistry

Primary human samples were postfixed and processed, and immunohistochemistry was performed on 10-μm-thick cryostat sections as previously shown (28, 31, 33). Tissue sections were stained according to manufacturer's instructions (see Supplementary Methods). Cell nuclei were counterstained by DAPI (Sigma-Aldrich). Negative controls were obtained by omitting primary antibody. TPCs were seeded onto Cultrex (Trevigen)-coated glass coverslips and staining was performed as described earlier (28, 31, 33). Fluorescent images, $n = 5$ fields/each independent lines, were obtained using a Zeiss Axioplan2 Microscope and Leica DMIRE2 Confocal Microscope.

In vitro invasion assays

Invasion assays were performed in 6-well Transwell chambers as shown (34). The upper side of the filters was coated with Cultrex (Trevigen) and 2×10^5 cells were seeded onto the layer of Cultrex in DMEM/F12 mitogen-free medium. Two weeks after plating, cells on the upper side of the filters were mechanically removed, and those migrated onto the lower side were fixed and stained by using the Hemacolor Rapid Staining Kit (Merck Millipore). The number of cells migrated through the Cultrex layer was scored by microscopy.

siRNAs, transfection, and quantifying gene silencing

siRNAs, transfection, and the quantification of gene silencing were performed according to manufacturer's instructions (see Supplementary Methods).

Cell sorting analysis

For cell sorting analysis, 3×10^6 cells per sample were identified, electronically gated on forward and orthogonal light scatter signals, sorted and analyzed with MoFlo XDP (Beckman Coulter) and with Summit V5.2 software (Beckman Coulter). Events representing cells binding anti-Wnt5a were identified by their light scatter and fluorescent signatures. Background fluorescence was estimated by substituting primary antibodies with specific isotype controls. Autofluorescence was also measured for each condition tested.

RNA quantitation, microarray, and data analysis

Total RNA both from tissue samples and from cells was extracted using the RNeasy Mini Kit (Qiagen). cDNA was synthetized using SuperScript III (Invitrogen). Relative gene expression was measured by real-time PCR as described (33), quantitative PCR reactions were run in duplicate and normalized to GAPDH as endogenous control. Whole human brain tissue RNA (WHB, Ambion, Invitrogen) or hNSCs employed as controls. RNA expression profiling was performed using Affymetrix GeneChip Human Transcriptome Array 2.0 (see Supplementary Methods). Raw transcriptome data were deposited in the GEO repository (accession number: GSE76422). Expression data analysis was performed using R and the Partek Genomics Suite package ver. 6.6. Low-level analysis and normalization were done using the *GCRMA* R package of Bioconductor and Partek. Biologic function and pathway analysis were conducted using Ingenuity Pathway Analysis (IPA; Qiagen).

In vivo evaluation of tumorigenicity

Tumorigenicity was determined by injecting hGBM TPCs into the right striatum of *Scid/bg* mice (Charles River Laboratory) as described (28). All animal procedures were conducted in accordance with the Guidelines for the Care and Use of Laboratory Animals and approved by the ethics board of the University of Milan Bicocca (Prot. 111). For assays of tumor initiation, 3 μL of a 1.5×10^4, 5×10^3, 2.5×10^3 of Wnt5a-purified cell fractions were injected orthotopically. Mice were infused with co- and post-treated paradigms as previously described (see Supplementary Methods; ref. 28). Tumor formation and growth were indirectly calculated once per week by sequential images taken with In Vivo Lumina (Xenogen, Caliper Life Sciences) as described previously (33, 35). Mice were sacrificed at different times comprised between 4 and 12 weeks postinjection, according to the cell line originally injected.

Analysis of dataset

We took advantage of the cBioPortal for Cancer Genomics (http://www.cbioportal.org/faq.jsp) and the TCGA brain cancer database (actually NIH GDC Legacy Archive: https://gdc-portal.nci.nih.gov/legacy-archive) containing –omic data (transcriptional, mutational, DNA methylation, and CNV) of 617 patients with glioblastoma. Data analysis depended on the availability of data files and clinicopathologic information. Significance was assessed both using web interfaces (GISTIC 2.0, cBioportal mutations pipeline) and statistical tests (ANOVA, Wilcoxon).
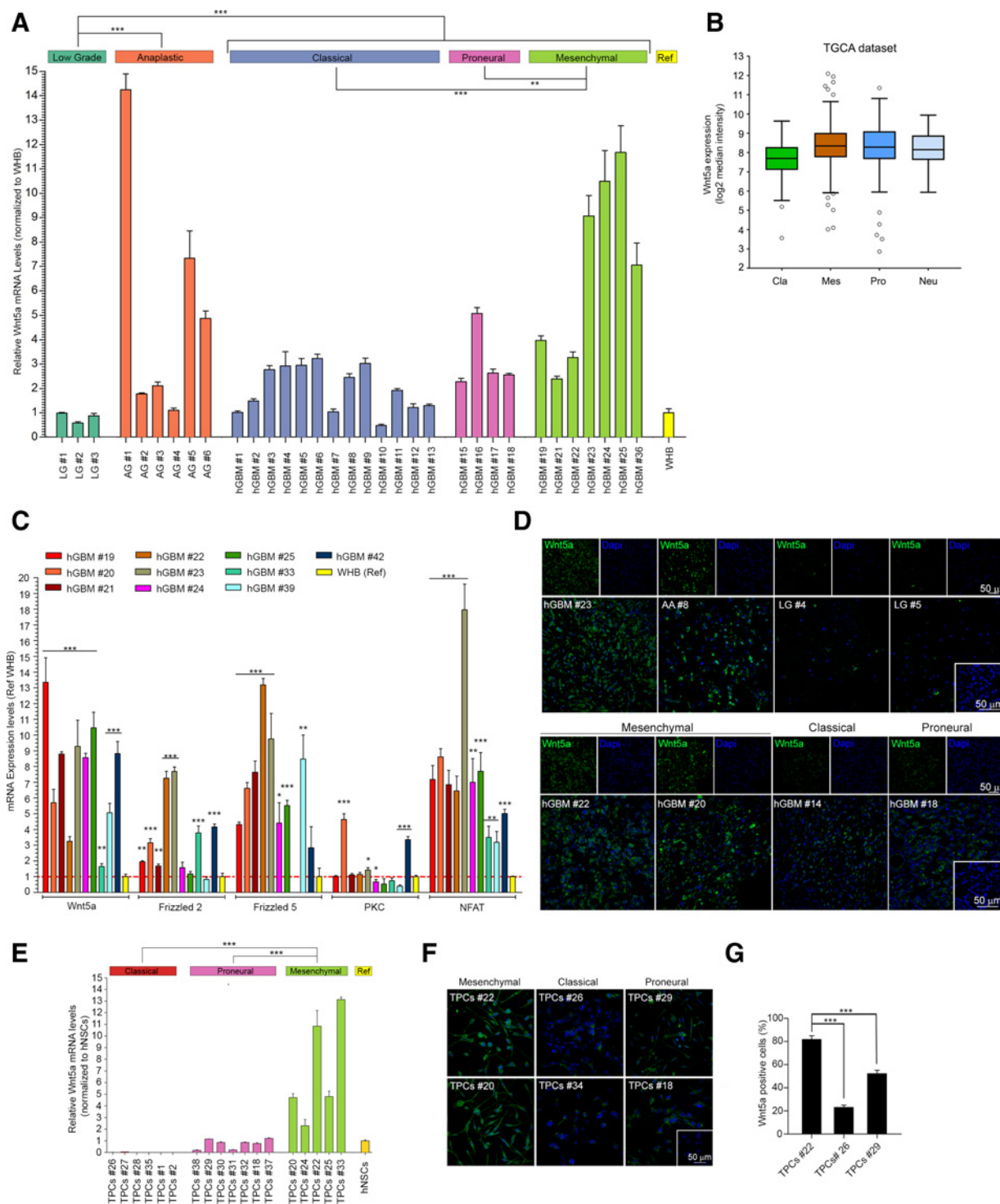
Binda et al.

Figure 1.
Wnt5a expression correlates with grading and hGBM subtypes in patients' specimens and their TPCs. **A,** Higher Wnt5a mRNA levels as detected by qPCR in anaplastic gliomas (AG; $n = 6$) and hGBM ($n = 24$) as compared with low-grade gliomas (LG; $n = 3$) and with whole human brain (WHB). ***, $P < 0.0001$, Student t test. Among hGBMs, mesenchymal tissues ($n = 7$) display significantly higher Wnt5a expression versus classical ($n = 13$) and proneural subtypes ($n = 4$). ***, $P < 0.0001$; **, $P = 0.013$, Student t test. **B,** Within the TCGA dataset, Wnt5a expression is significantly higher in the mesenchymal hGBM subtype (Mes; $n = 153$) than in the classical (Cla; $n = 139$; $P < 0.001$, Wilcoxon) rather than in the proneural (Pro; $n = 97$; $P = 0.6439$, Wilcoxon). **C,** Expression levels of the genes associated with the Wnt-Ca^{2+} pathway in mesenchymal hGBM tissues versus WHB, as determined by qPCR. *, $P < 0.05$; **, $P < 0.01$; ***, $P < 0.001$, pooled variant t test. (*Continued on the following page.*)

Statistical analysis

For *in vitro* studies, statistical tests were performed using GraphPad Prism v5.0 software, and ANOVA or Student *t* test according to the variance and distribution of data. Differential gene expression from microarray data was assessed by the implementation of the ANOVA test available in Partek Genomic Suite 6.6 with Benjamini–Hochberg false discovery rate (FDR) < 0.05. Because of the deviation from the normality distribution assumption, raw gene expression values of both cell lines and tissues were $\log_2$-transformed, beforehand. *In vivo* survival curves were estimated using GraphPad Prism v5.0 software, using the Kaplan–Meier method, and the curves were compared by log-rank test. *In vivo* comparisons between treated and control mice were carried out with a hierarchical linear model for repeated measurements as in (36). A 5% cutoff was used to validate result significance.

Results

Wnt5a overexpression in the most infiltrative high-grade gliomas and their TPCs

In agreement with previous observations (23), quantitative real-time analysis (qPCR) confirmed Wnt5a overexpression in the most infiltrative malignant glioma such as hGBMs and anaplastic gliomas but was not observed in low-grade gliomas (37) when compared with normal tissues (Fig. 1A and Supplementary Table S1). When dissecting the hGBM expression profiles further, Wnt5a mRNA levels can be used to categorize hGBMs tissues into the known subgroups (Fig. 1A and Supplementary Fig. S1A; ref. 38), even though there was no significant correlation with copy number alterations (Supplementary Table S2). These data were confirmed by analysis of public datasets (Supplementary Fig. S1B and S1C and Cancer Genome Atlas, TCGA, Research Network, 2013, data). Furthermore, in the TCGA dataset, significant Wnt5a overexpression was found in the mesenchymal subtype as compared with the classical one (Fig. 1B). This overexpression did not correlate with differences in the methylation profiles of the *WNT5A* gene (Supplementary Fig. S1D). Across independent datasets, Wnt5a was also a predictor of poor prognosis (Supplementary Fig. S1E). Strikingly, the expression levels of the genes associated with the Wnt-Ca^{2+} signaling pathway were higher in tissues from mesenchymal hGBMs, which are endowed with higher aggressiveness and invasiveness (38–40) as compared with healthy brain tissues (Fig. 1C).

These results were further confirmed when monitoring protein expression. Experiments that assessed Wnt5a immunostaining in malignant and low-grade glioma specimens reiterated that high Wnt5a expression was associated with the most infiltrative gliomas (Fig. 1D). Intense and widespread Wnt5a immunolabeling was retrieved in many cells of mesenchymal hGBM tissues as compared with few positive cells in the proneural and classical ones (Fig. 1D).

The same pattern of elevated Wnt5a expression observed in tissues derived from different hGBM subgroups was identified in their TPCs. Thus, TPCs from the mesenchymal subcluster had the highest expression of Wnt5a protein and mRNA as compared with cells from classical and proneural hGBMs (Fig. 1E–G; refs. 41–43). In contrast, the classical TPCs type predominantly expressed canonical Wnt3a (Supplementary Fig. S1F).

### Wnt5a drives the phenotypic change of cancer stem cells to high infiltrative potential

To determine whether Wnt5a exerts its biologic actions on the TPC population and to define the nature of such effects, we assessed the invasive capacity of TPCs from different hGBM subsets on Matrigel-coated membranes, *in vitro*. As expected, mesenchymal TPCs invaded much more efficiently than those from classical and proneural lineages (Fig. 2A and B). The invasive potential was Wnt5a-dependent, as inhibition of Wnt5a signaling by a Wnt5a blocking antibody (W5a-Ab; ref. 44), by an endogenous Wnt5a antagonist (the secreted frizzled-related protein 1, SFRP1), or by siRNA-mediated *WNT5A* silencing reduced hGBM TPCs migration through the Transwell (2-fold reduction in invasive cells; Fig. 2A–D, Supplementary Fig. S2A, S2B, S2E and data not shown). Interestingly, the different invasive potential among the different TPCs subclusters was inversely correlated to their inherent rate of amplification *in vitro*, in agreement with the "grow or go" model (Fig. 2E; ref. 45).

Notably, Wnt5a alone could modify the overall hGBM TPCs intrinsic invasive phenotype. In fact, when less infiltrating classical TPCs were treated with an exogenous recombinant human Wnt5a protein (rhWnt5a) or when stable *WNT5A* overexpression was induced, an exacerbated invasive phenotype was acquired. Thus, not only did the *in vitro* migratory capability increase to levels that far exceeded that of their empty vector-infected siblings but also these modified cells exhibited the invasive potential that is normally observed in naïve mesenchymal TPCs (Fig. 2F and G). Similar results were observed when proneural hGBM TPCs were treated with rhWnt5a or when stable *WNT5A* overexpression was induced (Supplementary Fig. S2C and S2D). Most important, the acquisition of exacerbated invasiveness in classical hGBM cells upon these treatments was associated to the acquisition of a "highly migratory" gene expression signature (Fig. 2H and Supplementary Table S3).

Altogether, these findings demonstrate that activation of the noncanonical Wnt5a pathway drives infiltrative potential in hGBM TPCs. More importantly, Wnt5a stimulation alone can trigger a global phenotypic switch in those hGBM TPCs that inherently possess a limited invasive ability. Upon Wnt5a stimulation, these TPCs acquire novel functional and molecular phenotypes, typical of the most infiltrative mesenchymal TPCs.

(*Continued.*) **D,** Immunolabeling of surgery specimens showing intense Wnt5a immunoreactivity (green) in hGBM (GBM#23) and anaplastic astrocytoma (AA#8) tissues as compared with few Wnt5a immunoreactive cells in low-grade samples (LG#4 and LG#5; top). Bottom, confocal immunolabeling showing that mesenchymal hGBM tissues (GBM#22 and GBM#20) display much more intense and widespread Wnt5a immunoreactivity versus classical (GBM#14) and proneural (GBM#18) ones. **E,** Higher Wnt5a expression in mesenchymal hGBM TPCs ($n = 5$), as detected by qPCR, versus classical ($n = 6$) and proneural ($n = 7$) TPCs. ***, $P < 0.0001$, Student *t* test. **F,** Strong immunolabeling for Wnt5a in mesenchymal TPCs (TPCs#22 and #20) as compared with weaker and infrequent signal in classical (TPCs#26 and #34) and proneural (TPCs#29 and #18) lines. **G,** Quantification of Wnt5a expression shown in **F**. ***, $P < 0.0001$ versus classical; ***, $P = 0.0003$ versus proneural TPCs, 2-tailed χ^2 test with continuity correction. Scale bar in **D, F**, 50 μm. Insets, no primary antibody as control. **A, C, E, G**, mean ± SEM from at least three independent experiments.

Binda et al.
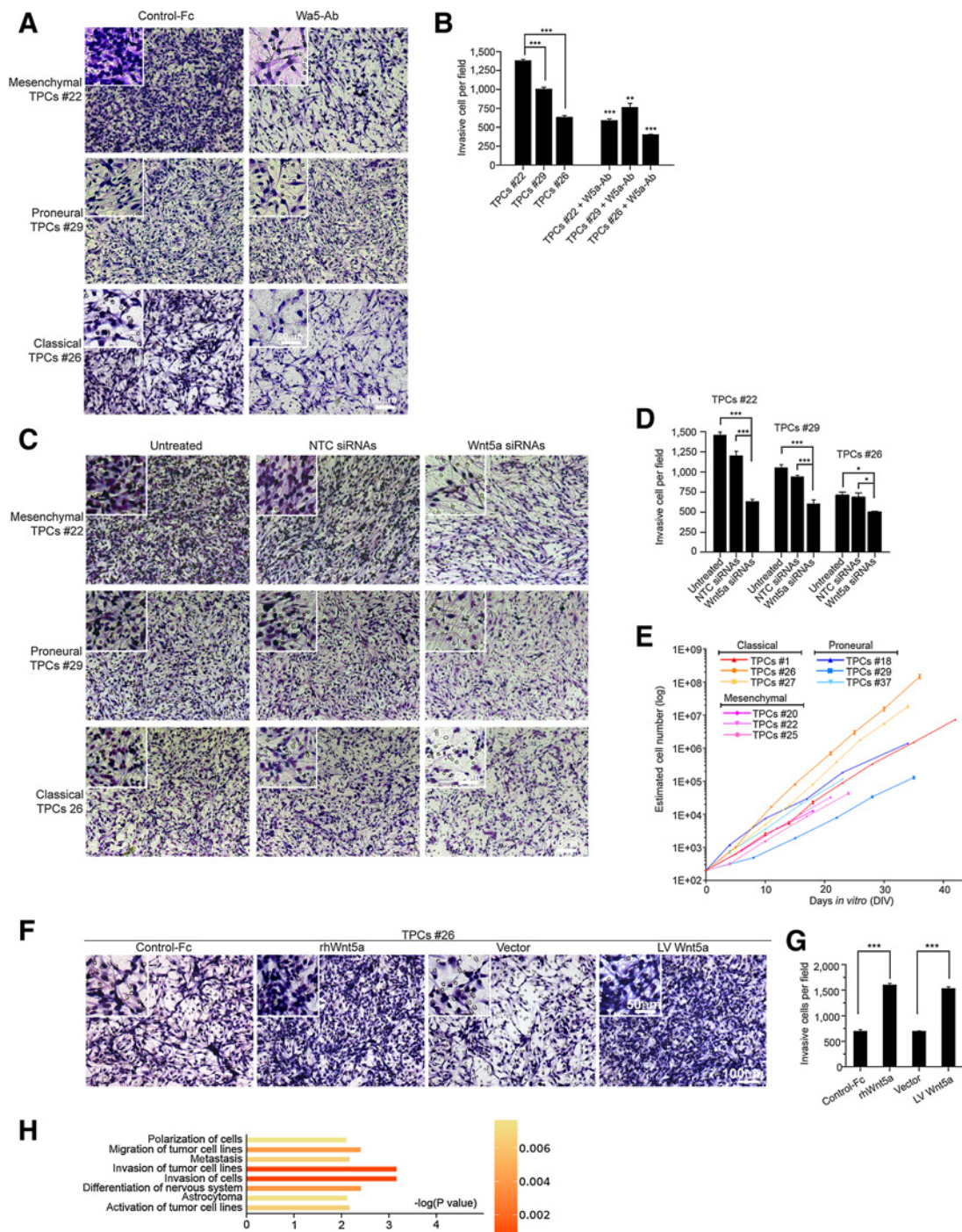
Figure 2.

Wnt5a overexpression drives invasive ability in hGBM TPCs. **A,** *In vitro* invasion assay showing that mesenchymal TPCs migrate more efficiently than proneural and classical lines (top to bottom, left). Cells were seeded in mitogen-free medium onto the upper side of the filters coated with Cultrex and the number of cells migrated through the Cultrex scored after 2 weeks. By administration of Wnt5a-blocking antibody (W5a-Ab, 2 μg/mL; middle), the migration of all three kinds of TPCs is lessened. **B,** Quantification of TPCs migration shown in **A**, Student t test. ***, $P < 0.0001$ versus mesenchymal and classical; **, $P = 0.023$ versus proneural control TPCs. **C,** TPC migration decrease is concomitant with siRNA-mediated Wnt5a downregulation. Quantification is shown in **D**. **, $P = 0.001$; ***, $P < 0.0001$, one-way ANOVA. **E,** Differences in the growth kinetics were detected among classical, mesenchymal, and proneural TPCs, with the former characterized by fast growth rate and the latter comprising slowly dividing TPCs. **F,** Treating TPCs with rhWnt5a or inducing stable Wnt5a overexpression (LV-Wnt5a) enhances the migration of classical TPCs (#26) versus Control-Fc or empty vector–infected siblings. Quantification is shown in **G**. ***, $P < 0.0001$, Student t test. **H,** Ingenuity analysis reporting a "highly migratory" functional signature acquired by classical TPCs after stable Wnt5a overexpression. Bars are colored in shades of orange according to the different level of significance. Scale bar in **A, C, F**, 100 μm. Scale bar in insets (higher magnification), 50 μm. **B, D, G,** mean ± SEM from at least three independent experiments.

These findings indicate that *WNT5A* may function as a master switch gene for infiltration.

Wnt5a: an "apical" master role in the molecular regulatory network sustaining infiltration capacity in hGBMs

To determine whether a cogent correlation exists between increased Wnt5a levels and enhanced invasion, we sorted mesenchymal TPCs into 2 distinct populations expressing either high (Wnt5a^{High}) or low Wnt5a levels (Wnt5a^{Low}; Fig. 3A). *In vitro* migration assays showed that Wnt5a^{High} TPCs invaded more efficiently than their Wnt5a^{Low} counterpart (2-fold increase in invasive cells; Fig. 3B and C). Most importantly, the exposure of Wnt5a^{Low} mesenchymal TPCs to rhWnt5a modified their phenotype to match that of their most infiltrative Wnt5a^{High} counterparts (Fig. 3D). This was also in agreement with experiments using glioma cells, whose invasive capacity was inherently nil, such as the U87 cell line. Forcing the overexpression of *WNT5A* was sufficient to bring about the expression an exacerbated infiltrative capacity (and an "infiltration-congruent" molecular signature) not only *in vitro* but also *in vivo* (Supplementary Fig. S3 and Table S4).

Next, we examined the transcription profiles of Wnt5a^{High} and Wnt5a^{Low} populations derived from mesenchymal hGBM tissues (Fig. 3E and F). Differential analysis of the transcriptional profiles demonstrated that the Wnt5a^{High} population expressed a distinctive infiltrative molecular program not observed in the Wnt5a^{Low} pool. In fact, the transcriptional modules of these 2 fractions were strikingly opposed when analyzing genes that control cell movement, homing, migration, and invasion (Fig. 3G and H and Supplementary Table S5). Also, most differentially expressed genes concerned pathways related to cell movement, migration, and invasion (Supplementary Fig. S4). Altogether, these data suggested that the key molecular properties that define the "infiltrative signature" in mesenchymal hGBM cells are restricted to the Wnt5a^{High} cell population.

In summary, these findings demonstrate that activation of the noncanonical Wnt5a pathway drives tissue migration and infiltration by hGBM TPCs. Strikingly, Wnt5a stimulation alone can trigger a global phenotypic switch in those hGBM TPCs that inherently possess limited invasive capacity. Upon stimulation of Wnt5a, these TPCs acquire both new molecular and functional phenotypes that are representative of the most infiltrative Wnt5a^{High} mesenchymal TPCs.

The Wnt5a-driven transition of TPCs to a highly infiltratory phenotype exacerbates their ability to invade the brain parenchyma

To reinforce the correlation between Wnt5a enhanced levels and the actual hGBM TPCs invasion ability in the brain parenchyma *in vivo* studies were performed. In agreement with our findings above, the xenografting of mesenchymal TPCs did establish intracranial hGBMs with a faster and broader infiltration pattern than those generated by classical or proneural TPCs (Fig. 4A). Mesenchymal hGBMs had cells that quickly spread from the graft site and dispersed extensively throughout the grey and white matter. In addition, the migratory cell population rapidly colonized the proximal brain hemisphere migrating along the fibers of the corpus callosum, the anterior commissure, and internal capsule (Fig. 4A and Supplementary Fig. S5A). The heightened invasive potential was tightly asso-

ciated with the Wnt5a^{High} mesenchymal TPCs pool (Fig. 4B). In contrast, the mesenchymal Wnt5a^{Low} TPCs gave rise to larger, yet more defined neoplastic masses that remained localized to the ipsilateral hemisphere, reminiscent of hGBM xenografts derived from classical TPCs (Fig. 4B). When classical TPCs were transduced with a *WNT5A* expression vector, in line with their "molecular fingerprint" (Fig. 2H), they exhibited an unusual migration, which was active along the fibers of the corpus callosum with an enhanced lateral spread within the parenchyma, a result that was comparable to that of mesenchymal TPCs (Fig. 4C). Furthermore, the highly invasive cells that reached the contralateral hemisphere in our TPC-established xenografts retained their inherent TPC characteristics. In fact, upon their isolation from the controlateral hemisphere, cells preserved the functional and molecular stem-like properties of the original mesenchymal or classical TPCs used to establish the xenograft in ipsilateral striatum (Supplementary Fig. S5B and S5C). Notably "contralateral" TPC neurospheres could be isolated from mesenchymal TPC-induced tumors significantly earlier than in tumors from classical ones—3 and 30 days posttransplant, respectively. These findings clearly demonstrate that Wnt5a drives TPCs invasiveness in an *in vivo* setting and can trigger a phenotypic state transition of the less infiltrating TPCs (Wnt5a^{Low} TPCs), to the most aggressive, invasive phenotype.

Inhibition of Wnt5a hinders brain parenchyma infiltration by hGBMs

The findings above strongly point to the hypothesis that Wnt5a may be a powerful therapeutic target for hGBM to further brain invasion by glioma cells.

We assessed this hypothesis by inhibiting Wnt5a activity in hGBM xenografts in an intracranial preclinical model. Immediately after orthotopic implantation of mesenchymal hGBM TPCs into immunodeficient *Scid* mice (28, 46), Wnt5a activity was antagonized for 2 weeks by the intraparenchymal infusion (33) of either W5a-Ab or a Wnt5a-derived hexapeptide (PepA), both capable of inhibiting Wnt5a-induced protein kinase C and Ca^{2+} signaling (47). Both treatments significantly decreased the size of the mesenchymal TPC–derived, intracranial hGBMs as compared with control animals (Fig. 5A). Remarkably, 9 weeks following transplantation and 7 weeks after the cessation of inhibitor infusion, the tumors receiving W5a-Ab or PepA were still significantly less spread as compared with controls. Furthermore, 12 weeks after infusion had ceased, intracranial invasion remained considerably reduced, which also resulted in significantly increased survival. Kaplan–Meier analysis revealed a median survival of 175 and 173 days for mice receiving W5a-Ab and PepA, respectively, versus 134 days for controls (Fig. 5B), confirming the therapeutic efficacy of W5a-Ab and PepA administration. Interestingly, these effects were not restricted to the mesenchymal hGBMs. To a lesser extent than for xenografts derived from the mesenchymal cluster, classical TPC-derived hGBMs do possess the capacity to infiltrate, which is of cogent clinical relevance. The spreading of xenograft tumors established from classical hGBM TPCs was also significantly reduced when treated with intraparenchymal infusion of either W5a-Ab or PepA (Fig. 5C). This reduction in migratory ability was even more apparent when classical TPCs were allowed to establish sizeable tumors (33) prior to the infusion of PepA or W5a-Ab (Fig. 5D; ref. 33). Similar

Binda et al.
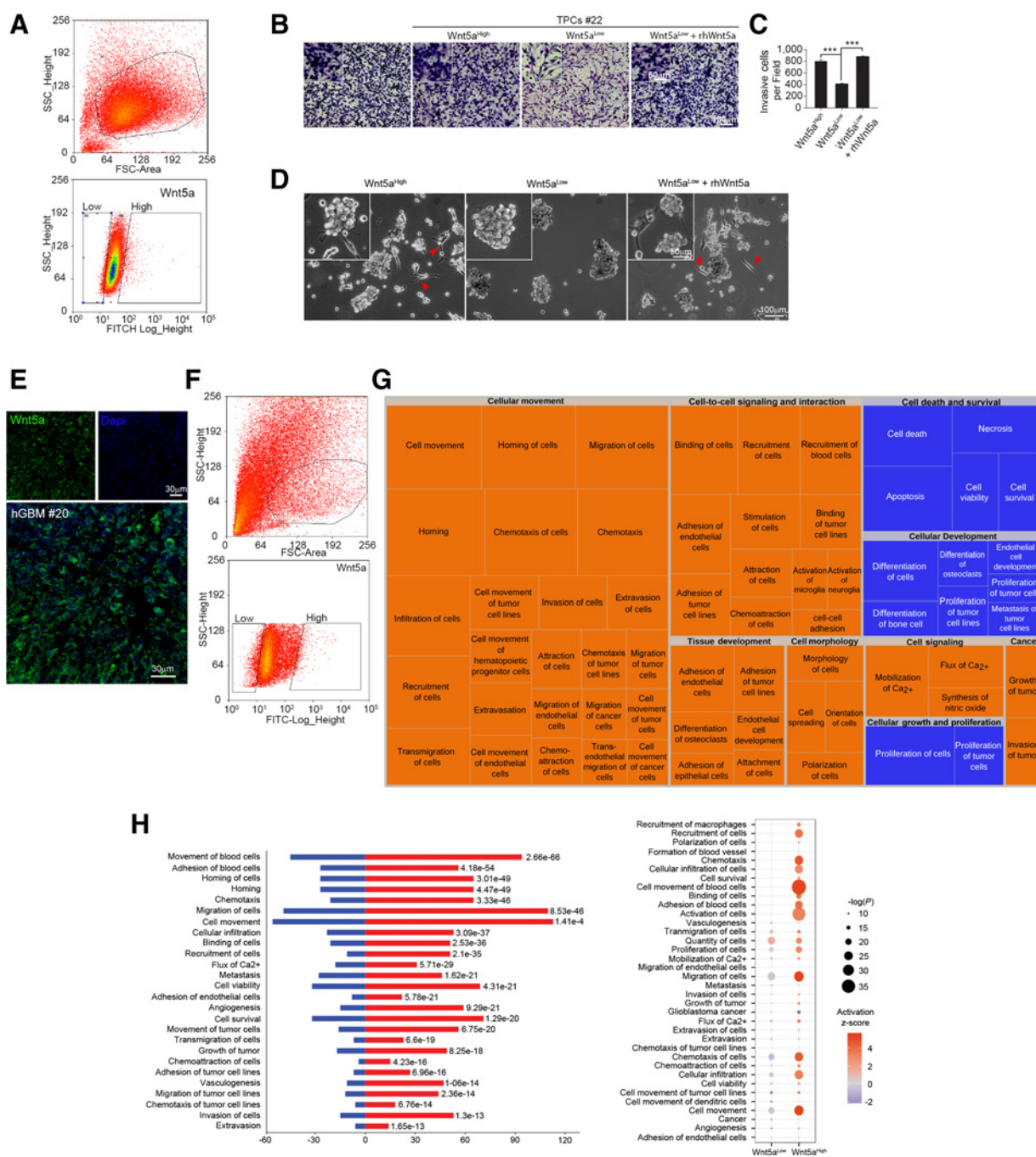
Figure 3.
Elevated Wnt5a levels in brain tumor cells correlate with activation of functional and molecular programs that underpin invasive potential. **A,** Mesenchymal TPCs were gated and sorted according to Wnt5a expression. **B,** When treated with exogenous rhWnt5a, Wnt5a^{Low} cells acquire an unprecedented ability to migrate, quantitatively matching that of Wnt5a^{High} siblings. Quantification of this phenomenon is shown in **C**, mean ± SEM. ***, $P < 0.0001$, Student t test. **D,** Phase-bright microphotographs of neurospheres showing that Wnt5a^{Low} cells display typical rounded morphology as compared with more heterogeneous cell populations in both Wnt5a^{High} and rhWnt5a-treated Wnt5a^{Low} cultures, characterized by many protruding bipolar cells (red arrowheads), indicative of enhanced cell adhesion and migration. **E** and **F,** Example of mesenchymal hGBM specimen (GBM#20) immunostained for Wnt5a (**E**), gated and sorted according to Wnt5a expression (**F**). **G,** IPA shows that most overactivated cellular functions in the Wnt5a^{High} population belong to cell movement and migration (orange), unlike the Wnt5a^{Low} pool. The latter is characterized by enrichment in cell apoptosis, proliferation, and differentiation functions (blue). The higher the statistical significance, the bigger the rectangles. **H,** When compared with Wnt5a^{Low} siblings, genes upregulated in Wnt5a^{High} cells are mostly related to biological functions as cell movement, homing, and migration (left). Red and blue bars count for up- and downregulated genes, respectively. Right, even by comparing Wnt5a^{High} and Wnt5a^{Low} fractions with the unsorted, original population, the overrepresented genes and their biological functions in the Wnt5a^{High} pool were mostly associated with cell movement, migration, and invasion. The positive z-scores mean functional activation. Scale bar in **B**, **D**, 100 μm. Insets, higher magnification. Scale bar, 50 μm.
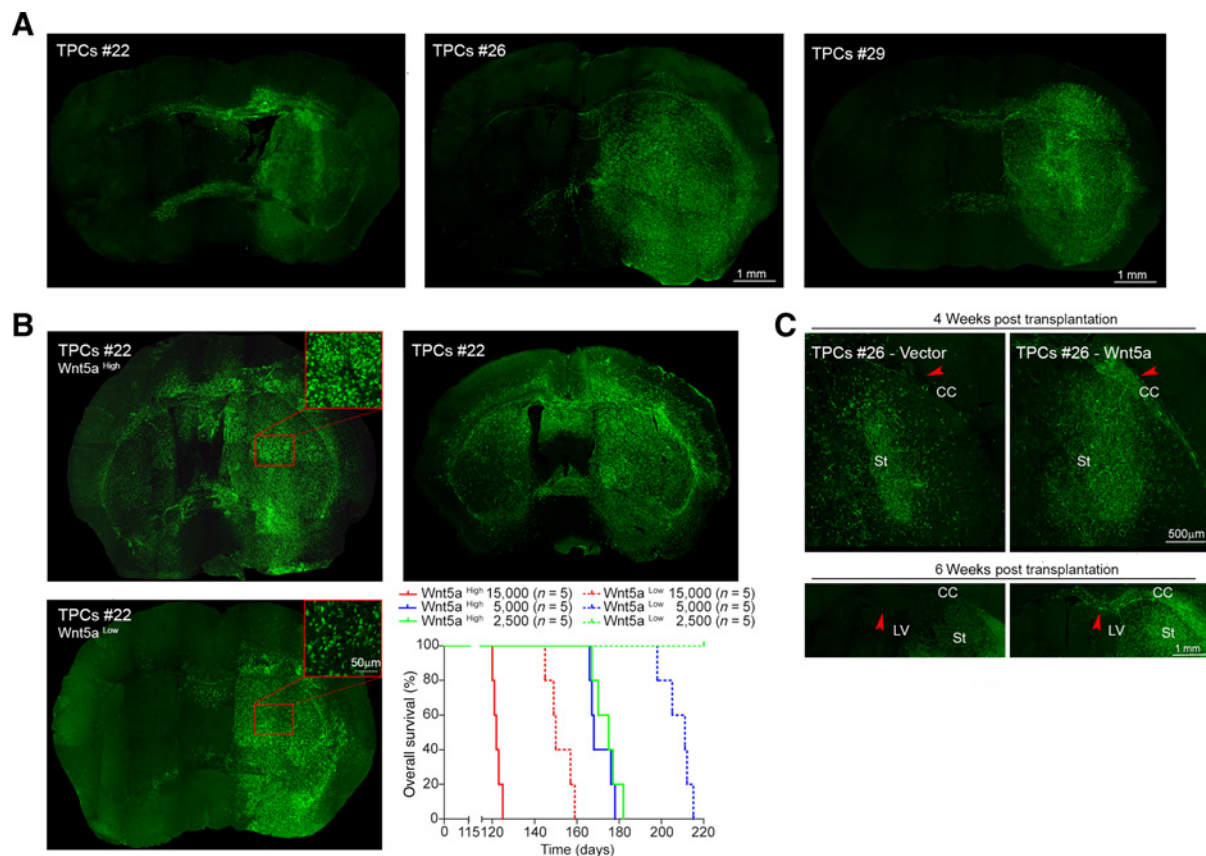
Figure 4.
Wnt5a levels influence dispersal of hGBM TPCs *in vivo*. **A,** Serial histologic reconstruction shows that at 8 weeks following implantation, luciferase-tagged mesenchymal TPCs (luc-TPCs; left, TPCs#22) form smaller tumor masses but display a broader invasion pattern as compared with classical (middle, TPCs#26) and proneural TPCs (right, TPCs#29). $n = 5$ mice per groups. Scale bar, 1 mm. **B,** Brain sections showing that the Wnt5a^{High} TPC pool is the most invasive since, in only 12 weeks following implantation, as few as 1.5×10^4 cells established tumors (top, left) as extended as those established by 20 fold more (3×10^5) unsorted mesenchymal TPCs (TPCs#22; top, right). When implanting 1.5×10^4 Wnt5a^{Low} mesenchymal TPCs (bottom, left), more compact masses were generated, resembling classical TPCs (compare with **A**, middle). $n = 5$ mice per groups. Scale bar, 1 mm. Insets, higher magnification. Scale bar, 50 μm. Bottom right, Kaplan–Meier survival curves demonstrating that mice receiving 1.5×10^4, 5×10^3, or 2.5×10^3 Wnt5a^{High} TPCs die earlier than those implanted with similar amounts of Wnt5a^{Low} cells, Mantel–Cox and Breslow–Wilcoxon tests, log-rank $P < 0.0001$, $n = 5$ mice per groups. **C,** When classical TPCs (TPCs#26-empty; left) were forced to overexpress Wnt5a (TPCs#26-Wnt5a; right), in 4 and 6 weeks established tumors whose spreading was significantly enhanced, migrated along the fibers of the corpus callosum much faster than those generated by empty vector–infected cells (red arrowheads). Scale bars, 500 μm and 1 mm.

results were observed in xenografts from proneural hGBM TPCs (Fig. 5E and F).

Discussion

In this work, we demonstrate that it is the level of expression of Wnt5a that defines the infiltrative capacity of human glioma cells and that, by itself, Wnt5a bestows an exacerbated invasive phenotype upon these cells by activation of a complement of functional and molecular characteristics. One of the most prominent cell targets of exacerbated Wnt5a activity is the tumor-initiating glioma TPC pool. By antagonizing Wnt5a activity in this cell population, the invasive potential is vastly reduced. These findings suggest that significant, therapeutic beneficial effects can be gleaned for intracranial hGBM.

The expression of Wnt5a is known to be upregulated in human gliomas (23). Findings on Wnt5a roles and functions in these tumors are restricted to the observed increased motility in cultured cell lines (25, 27). Recently, however, it has been shown that the enhanced migration caused in hGBMs by reduced Wnt inhibitor 1 activity is mediated by Wnt5a (48). We now demonstrated that Wnt5a functions as a master regulator in determining the prototypical invasive glioma potential in hGBMs, particularly, in their TPCs.

First, we show that Wnt5a overexpression is, in fact, a defining feature of the most infiltrating malignant gliomas, that is, anaplastic gliomas and hGBMs (23). In the latter, not only are the highest Wnt5a levels found in the mesenchymal phenotype—which has been associated with tumor aggressiveness and elevated invasive potential (38–40, 49)—but Wnt5a expression can even be used to categorize hGBMs tissues into the known subgroups (38). Second, the strong tie between invasiveness and Wnt5a overexpression is directly connected with cancer stem–like hGBM TPCs. Wnt5a expression was found to be from 10- to 1,000-fold higher in mesenchymal hGBM TPCs when compared with TPCs derived from the

Binda et al.
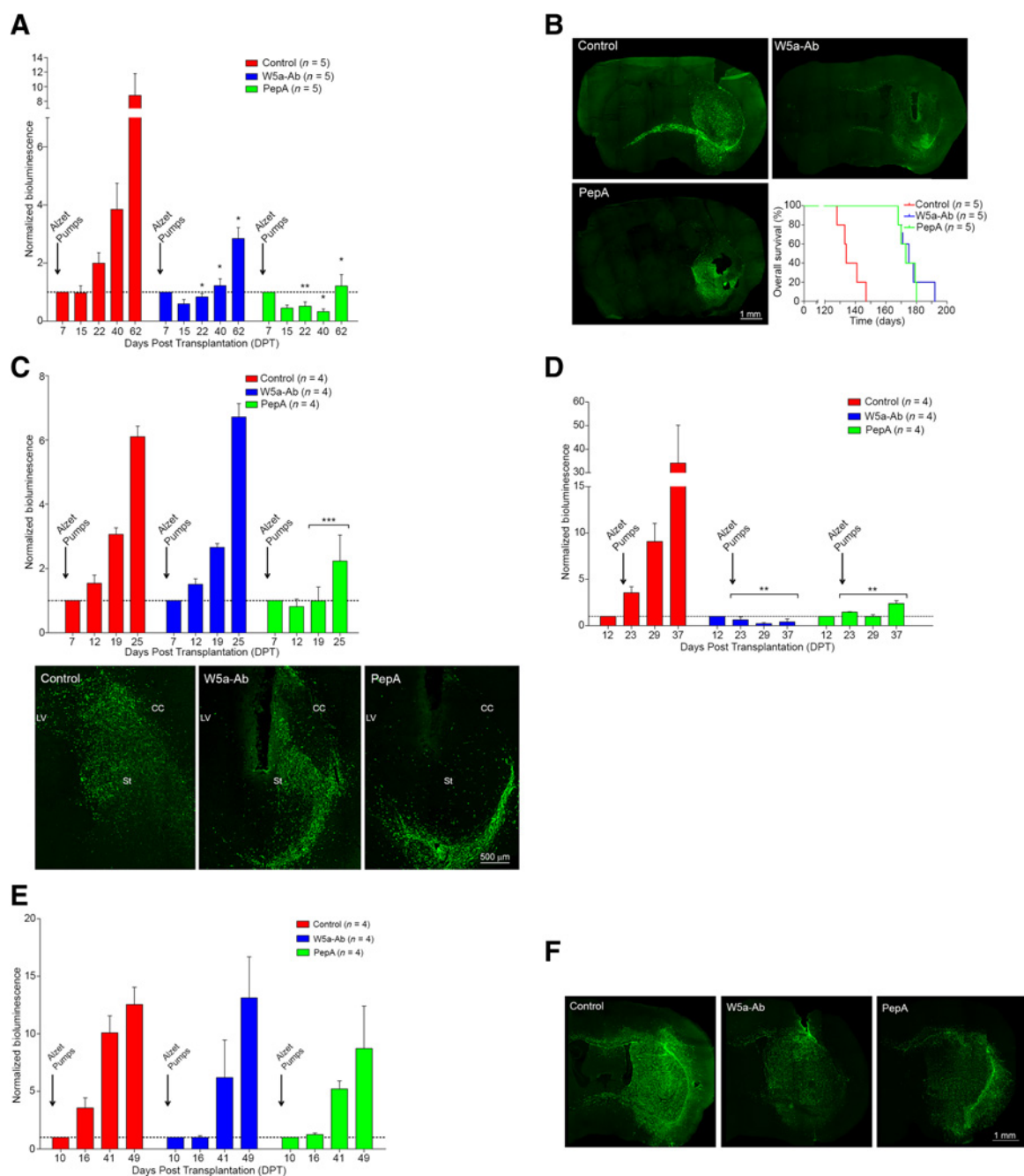
Figure 5.

In vivo inhibition of Wnt5a activity impairs brain invasion. **A,** hGBM xenografts from mesenchymal luc-TPCs infused with either W5a-Ab or PepA display reduced tumor growth as compared with controls, as shown by quantitative time course imaging analysis, *, $P < 0.05$; **, $P < 0.01$ versus control hierarchical linear model for repeated measures; $n = 5$ mice per groups. **B,** Brain sections from experiment A show that the tumors infused with W5a-Ab and PepA spread significantly less than controls. Bottom right, Kaplan–Meier plot of overall survival showing that mice treated with Wnt5a inhibitors survived significantly longer than controls, Mantel–Cox and Breslow–Wilcoxon tests, log-rank Wnt5a-Ab $P = 0.0006$, PepA $P = 0.025$ versus control; $n = 5$ mice per groups. Scale bar, 1 mm. **C,** While W5a-Ab was ineffective, PepA limited the growth of tumors established by classical TPCs as compared with control (top). ***, $P < 0.001$ hierarchical linear model for repeated measures; $n = 4$ mice per groups. Bottom, Serial histological reconstruction showed that W5a-Ab or PepA infusion reduced the spread of classical luc-TPC versus control (25 days posttransplantation; DPT), although the effect of W5a-Ab was less intense. CC, corpus callosum; LV, lateral ventricle; St, striatum. Scale bar, 500 µm. **D,** By infusing either W5a-Ab or PepA with the posttreatment regimen, signal from classical-luc TPCs was significantly reduced versus control tumors. **, $P < 0.01$, hierarchical linear model for repeated measures. $n = 4$ mice per groups. **E,** By implanting proneural luc-TPCs, the overall F-luc signal intensity using either W5a-Ab or PepA was not reduced. ns, nonsignificant; $n = 4$ mice per groups. **F,** Immunohistochemical reconstruction revealed that spreading of tumors established by proneural TPCs was inhibited by Wnt5a-Ab or PepA versus control tumors (41 DPT). Scale bar, 1 mm. **A**, **C**, **D**, **E**, mean ± SEM; arrows mark the starting point of infusion.

proneural and classical clusters—a reversed pattern as compared with that of the Wnt5a antagonist Wnt3a (16). In addition, the mesenchymal Wnt5a^{High} TPC fraction, but not its Wnt5a^{Low} counterpart, displayed considerable invasive capability, in vitro and in vivo. Finally, a direct correlation was observed between Wnt5a levels and the invasive potential, which demonstrated that Wnt5a overexpression is a driving factor behind glioma TPCs infiltrative ability as a whole. In fact, the observed difference between Wnt5a^{High} and Wnt5a^{Low} TPCs in their ability to migrate could be abolished when the Wnt5a pathway was activated in Wnt5a^{Low} cells (Figs. 3B and C and 4B). As expected, the very opposite phenomenon took place when Wnt5a activity was antagonized in TPCs from all hGBM subgroups, resulting in the ablation of their migratory ability (Figs. 2A–D and 5). These findings clearly demonstrate that diverse Wnt5a expression levels can confer distinct inherent invasive ability to the different hGBMs and their TPCs.

A major discovery in this work was the fact that Wnt5a drives acquisition of the glioma TPCs' exacerbated infiltrating phenotype by globally overhauling the infiltrative molecular program of these cells. It has been demonstrated previously that the invasive behavior exhibited by glioma cells hinges on the coordinated activation of multiple cell signaling pathways (3, 5, 50). For the most aggressive TPC cells, that is, those of the mesenchymal hGBM cluster, this translates into a specific signature in which cell motility, migration, and aggressiveness pathways are enriched (39, 40, 49). Our analysis identified this molecular module in highly invasive Wnt5a^{High} mesenchymal TPCs but not in their less infiltrating Wnt5a^{Low} siblings.

Neither mesenchymal Wnt5a^{Low,} nor classical TPCs expressed genes that gave rise to an "invasive" signature. Yet, when WNT5A levels were increased in both these TPCs, not only was invasiveness enhanced to the level of their counterparts but also its expression concomitantly triggered the acquisition of an overall expression profile that matched the prototypical "infiltrative signature" of mesenchymal hGBM, particularly their Wnt5a^{High} TPCs. Such a strong association between high Wnt5a levels and the concomitant expression of both exacerbated infiltrating functional and molecular characteristics in TPCs demonstrates that Wnt5a is a key determinant of the invasive phenotype in hGBMs, particularly in their stem-like TPCs. This is consistent with the Wnt5a role as a membrane receptor ligand, which places it at an apical, hierarchic position in the ramified network of molecular pathways that underlies brain cancer cell infiltration. While our findings show that the overexpression of Wnt5a is particularly prominent in the hGBM subcluster the Wnt5a effects on glioma cell infiltration are to be seen as a general phenomenon, which takes place in all hGBM tumors.

The fact that Wnt5a overexpression might be associated to distinct degrees of invasiveness in various hGBM subtypes and their associated TPCs points to the existence of heterogeneous subpopulations of hGBM tumor–founding stem-like cells endowed with inherently different infiltration capacities in these high-grade gliomas. This is demonstrated by the co-existence of Wnt5^{High} and Wnt5a^{Low} TPC pools inside the very same mesenchymal hGBM specimen that display dissimilar infiltrative fingerprints and capacities. Thus, the axiomatic heterogeneity that characterizes hGBMs at the cytohistologic level may extend to encompass disparateness in the intrinsic infiltrating capacity of these cancers' very founder cells. Of paramount importance is the observation that the differential

ability to invade is interconvertible and that the switch from a state to another can be accomplished, at both the functional and molecular levels, by simply manipulating Wnt5a levels in hGBM TPCs. A schematic that incorporates the above findings portrays a tentative model of how invasion may be regulated at the TPC level in hGBM is shown in Supplementary Fig. S6.

Also, of note is the observation that the fast infiltrating hGBM cells, that reach the hemispheres contralateral to the transplantation site in our orthotopic model, retain the prototypical features of stem-like TPCs of mesenchymal and classical clusters (Supplementary Fig. S5B and S5C). This reinforces the notion that properties of tumor-initiating cells actively support the lethal invasive process in hGBMs.

The critical, master role played by Wnt5a in regulating hGBM TPC physiology—the promotion of an infiltratory cell functionality and the initiation of the global invasive molecular expression signature—makes Wnt5a a promising target for therapeutic approaches that may antagonize the spreading of tumor-initiating cells throughout the brain. When Wnt5a activity was attenuated in preclinical experimental conditions using orthotopic hGBM xenografts, the ability of the tumor mass to expand and migrate was significantly reduced. The peptide treatment was more effective, likely due to the ability of the small molecules to diffuse into the tissue much more efficiently than the larger antibody molecules. As expected, the beneficial effects were less evident in grafts established by the classical and proneural hGBM cells and most prominent in those arising from the most invasive mesenchymal TPCs.

Thus, anti-Wnt5a treatments have the potential to effectively prevent invasion of the brain parenchyma by hGBM cells, particularly TPCs, endowed with the ability to establish or re-establish the whole tumor at the single-cell level at a new site. As these experiments were conducted under preclinical conditions, these findings will be more rapidly applied in support of clinical trials and thus to the therapeutic setting. The availability of these approaches might pave the way to future, more efficacious combinatorial treatments, that combine approaches aimed at killing the cancerous cells or to hinder their proliferation with strategies that, simultaneously, limit the spreading of the tumor-initiating cells.

Disclosure of Potential Conflicts of Interest

A.L. Vescovi is an employee of HyeprStem SA and has ownership interest (including patents) in HyeprStem SA. No potential conflicts of interest were disclosed by the other authors.

Authors' Contributions

Conception and design: E. Binda, M. Carella, R. Duggal, A.L. Vescovi
Development of methodology: E. Binda, A. Visioli, F. Giani, N. Trivieri, S. Restelli, F. Di Meco, R. Duggal
Acquisition of data (provided animals, acquired and managed patients, provided facilities, etc.): F. Legnani, M. Carella, F. Di Meco
Analysis and interpretation of data (e.g., statistical analysis, biostatistics, computational analysis): E. Binda, O. Palumbo, F. Dezi, T. Mazza, C. Fusilli, M. Carella, A.L. Vescovi
Writing, review, and/or revision of the manuscript: E. Binda, F. Dezi, R. Duggal, A.L. Vescovi
Administrative, technical, or material support (i.e., reporting or organizing data, constructing databases): E. Binda, F. Di Meco
Study supervision: E. Binda, F. DiMeco, A.L. Vescovi
Other (performed experiments): A. Visioli, F. Giani, N. Trivieri, S. Restelli

Binda et al.

References

1. Delgado-López PD, Corrales-García EM. Survival in glioblastoma: a review on the impact of treatment modalities. Clin Transl Oncol 2016; 18:1062–71.
2. Chen J, Li Y, Yu TS, McKay RM, Burns DK, Kernie SG, et al. A restricted cell population propagates glioblastoma growth after chemotherapy. Nature 2012;488:522–6.
3. Nakada M, Nakada S, Demuth T, Tran NL, Hoelzinger DB, Berens ME. Molecular targets of glioma invasion. Cell Mol Life Sci 2007;64:458–78.
4. Giese A, Bjerkvig R, Berens ME, Westphal M. Cost of migration: invasion of malignant gliomas and implications for treatment. J Clin Oncol 2003; 21:1624–36.
5. Paw I, Carpenter RC, Watabe K, Debinski W, Lo HW. Mechanisms regulating glioma invasion. Cancer Lett 2015;362:1–7.
6. Mentlein R, Hattermann K, Held-Feindt J. Lost in disruption: role of proteases in glioma invasion and progression. Biochim Biophys Acta 2012;1825:178–85.
7. Roth W, Wild-Bode C, Platten M, Grimmel C, Melkonyan HS, Dichgans J, et al. Secreted Frizzled-related proteins inhibit motility and promote growth of human malignant glioma cells. Oncogene 2000; 19:4210–20.
8. Kahlert UD, Maciaczyk D, Doostkam S, Orr BA, Simons B, Bogiel T, et al. Activation of canonical WNT/β-catenin signaling enhances *in vitro* motility of glioblastoma cells by activation of ZEB1 and other activators of epithelial-to-mesenchymal transition. Cancer Lett 2012;325:42–53.
9. Smalley MJ, Dale TC. Wnt signalling in mammalian development and cancer. Cancer Metastasis Rev 1999;18:215–30.
10. Saran A. Medulloblastoma: role of developmental pathways, DNA repair signaling, and other players. Curr Mol Med 2009;9:1046–57.
11. de Bont JM, Packer RJ, Michiels EM, den Boer ML, Pieters R. Biological background of pediatric medulloblastoma and ependymoma: a review from a translational research perspective. Neuro Oncol 2008;10:1040–60.
12. MacDonald BT, Tamai K, He X. Wnt/beta-catenin signaling: components, mechanisms, and diseases. Dev Cell 2009;17:9–26.
13. Gong A, Huang S. FoxM1 and Wnt/β-catenin signaling in glioma stem cells. Cancer Res 2012;72:5658–62.
14. Wang K, Xie D, Xie J, Wan Y, Ma L, Qi X, et al. MiR-27a regulates Wnt/beta-catenin signaling through targeting SFRP1 in glioma. Neuroreport 2015;26:695–702.
15. Veeman MT, Axelrod JD, Moon RT. A second canon. Functions and mechanisms of beta-catenin-independent Wnt signaling. Dev Cell 2003;5:367–77.
16. Sato A, Yamamoto H, Sakane H, Koyama H, Kikuchi A. Wnt5a regulates distinct signalling pathways by binding to Frizzled2. EMBO J 2010; 29:41–54.
17. Logan CY, Nusse R. The Wnt signaling pathway in development and disease. Annu Rev Cell Dev Biol 2004;20:781–810.
18. Fernandez-Cobo M, Zammarchi F, Mandeli J, Holland JF, Pogo BG. Expression of Wnt5A and Wnt10B in non-immortalized breast cancer cells. Oncol Rep 2007;17:903–7.
19. Kurayoshi M, Oue N, Yamamoto H, Kishida M, Inoue A, Asahara T, et al. Expression of Wnt-5a is correlated with aggressiveness of gastric cancer by stimulating cell migration and invasion. Cancer Res 2006;66:10439–48.
20. Wang Q, Williamson M, Bott S, Brookman-Amissah N, Freeman A, Nariculam J, et al. Hypomethylation of WNT5A, CRIP1 and S100P in prostate cancer. Oncogene 2007;26:6560–5.
21. Ripka S, König A, Buchholz M, Wagner M, Sipos B, Klöppel G, et al. WNT5A–target of CUTL1 and potent modulator of tumor cell migration and invasion in pancreatic cancer. Carcinogenesis 2007;28:1178–87.
22. Da Forno PD, Pringle JH, Hutchinson P, Osborn J, Huang Q, Potter L, et al. WNT5A expression increases during melanoma progression and correlates with outcome. Clin Cancer Res 2008;14:5825–32.
23. Pu P, Zhang Z, Kang C, Jiang R, Jia Z, Wang G, et al. Downregulation of Wnt2 and beta-catenin by siRNA suppresses malignant glioma cell growth. Cancer Gene Ther 2009;16:351–61.
24. Yu JM, Jun ES, Jung JS, Suh SY, Han JY, Kim JY, et al. Role of Wnt5a in the proliferation of human glioblastoma cells. Cancer Lett 2007;257:172–81.
25. Habu M, Koyama H, Kishida M, Kamino M, Iijima M, Fuchigami T, et al. Ryk is essential for Wnt-5a-dependent invasiveness in human glioma. J Biochem 2014;156:29–38.
26. Kamino M, Kishida M, Kibe T, Ikoma K, Iijima M, Hirano H, et al. Wnt-5a signaling is correlated with infiltrative activity in human glioma by inducing cellular migration and MMP-2. Cancer Sci 2011;102:540–8.
27. Lee Y, Lee JK, Ahn SH, Lee J, Nam DH. WNT signaling in glioblastoma and therapeutic opportunities. Lab Invest 2016;96:137–50.
28. Galli R, Binda E, Orfanelli U, Cipelletti B, Gritti A, De Vitis S, et al. Isolation and characterization of tumorigenic, stem-like neural precursors from human glioblastoma. Cancer Res 2004;64:7011–21.
29. Lathia JD, Mack SC, Mulkearns-Hubert EE, Valentim CL, Rich JN. Cancer stem cells in glioblastoma. Genes Dev 2015;29:1203–17.
30. Dirks PB. Brain tumor stem cells: the cancer stem cell hypothesis writ large. Mol Oncol 2010;4:420–30.
31. Gritti A, Parati EA, Cova L, Frolichsthal P, Galli R, Wanke E, et al. Multipotential stem cells from the adult mouse brain proliferate and self-renew in response to basic fibroblast growth factor. J Neurosci 1996;16:1091–100.
32. Vescovi AL, Parati EA, Gritti A, Poulin P, Ferrario M, Wanke E, et al. Isolation and cloning of multipotential stem cells from the embryonic human CNS and establishment of transplantable human neural stem cell lines by epigenetic stimulation. Exp Neurol 1999;156:71–83.
33. Binda E, Visioli A, Giani F, Lamorte G, Copetti M, Pitter KL, et al. The EphA2 receptor drives self-renewal and tumorigenicity in stem-like tumor-propagating cells from human glioblastomas. Cancer Cell 2012;22:765–80.
34. Pennacchietti S, Michieli P, Galluzzo M, Mazzone M, Giordano S, Comoglio PM. Hypoxia promotes invasive growth by transcriptional activation of the met protooncogene. Cancer Cell 2003;3:347–61.
35. Jenkins DE, Hornig YS, Oei Y, Dusich J, Purchio T. Bioluminescent human breast cancer cell lines that permit rapid and sensitive *in vivo* detection of mammary tumors and multiple metastases in immune deficient mice. Breast Cancer Res 2005;7:R444–54.
36. Singer JD, Willett JB. Applied longitudinal data analysis: modeling change and event occurrence. Oxford; New York: Oxford University Press; 2003.
37. Louis DN, Perry A, Reifenberger G, von Deimling A, Figarella-Branger D, Cavenee WK, et al. The 2016 World Health Organization Classification of Tumors of the Central Nervous System: a summary. Acta Neuropathol 2016;131:803–20.
38. Verhaak RG, Hoadley KA, Purdom E, Wang V, Qi Y, Wilkerson MD, et al. Integrated genomic analysis identifies clinically relevant subtypes of glioblastoma characterized by abnormalities in PDGFRA, IDH1, EGFR, and NF1. Cancer Cell 2010;17:98–110.
39. Carro MS, Lim WK, Alvarez MJ, Bollo RJ, Zhao X, Snyder EY, et al. The transcriptional network for mesenchymal transformation of brain tumours. Nature 2010;463:318–25.
40. Brown DV, Daniel PM, D'Abaco GM, Gogos A, Ng W, Morokoff AP, et al. Coexpression analysis of CD133 and CD44 identifies proneural and mesenchymal subtypes of glioblastoma multiforme. Oncotarget 2015;6: 6267–80.

41. Sandberg CJ, Altschuler G, Jeong J, Strømme KK, Stangeland B, Murrell W, et al. Comparison of glioma stem cells to neural stem cells from the adult human brain identifies dysregulated Wnt- signaling and a fingerprint associated with clinical outcome. Exp Cell Res 2013;319:2230–43.

42. Chen R, Nishimura MC, Bumbaca SM, Kharbanda S, Forrest WF, Kasman IM, et al. A hierarchy of self-renewing tumor-initiating cell types in glioblastoma. Cancer Cell 2010;17:362–75.

43. Balbous A, Cortes U, Guilloteau K, Villalva C, Flamant S, Gaillard A, et al. A mesenchymal glioma stem cell profile is related to clinical outcome. Oncogenesis 2014;3:e91.

44. Parish CL, Castelo-Branco G, Rawal N, Tonnesen J, Sorensen AT, Salto C, et al. Wnt5a-treated midbrain neural stem cells improve dopamine cell replacement therapy in parkinsonian mice. J Clin Invest 2008;118:149–60.

45. Kathagen-Buhmann A, Schulte A, Weller J, Holz M, Herold-Mende C, Glass R, et al. Glycolysis and the pentose phosphate pathway are differentially associated with the dichotomous regulation of glioblastoma cell migration versus proliferation. Neuro Oncol 2016;18:1219–29.

46. Piccirillo SG, Reynolds BA, Zanetti N, Lamorte G, Binda E, Broggi G, et al. Bone morphogenetic proteins inhibit the tumorigenic potential of human brain tumour-initiating cells. Nature 2006;444:761–5.

47. Jenei V, Sherwood V, Howlin J, Linnskog R, Säfholm A, Axelsson L, et al. A t-butyloxycarbonyl-modified Wnt5a-derived hexapeptide functions as a potent antagonist of Wnt5a-dependent melanoma cell invasion. Proc Natl Acad Sci U S A 2009;106:19473–8.

48. Vassallo I, Zinn P, Lai M, Rajakannu P, Hamou MF, Hegi ME. WIF1 re-expression in glioblastoma inhibits migration through attenuation of non-canonical WNT signaling by downregulating the lncRNA MALAT1. Oncogene 2016;35:12–21.

49. Phillips HS, Kharbanda S, Chen R, Forrest WF, Soriano RH, Wu TD, et al. Molecular subclasses of high-grade glioma predict prognosis, delineate a pattern of disease progression, and resemble stages in neurogenesis. Cancer Cell 2006;9:157–73.

50. Cuddapah VA, Robel S, Watkins S, Sontheimer H. A neurocentric perspective on glioma invasion. Nat Rev Neurosci 2014;15:455–65.

Correction: Wnt5a Drives an Invasive Phenotype in Human Glioblastoma Stem-like Cells

In this article (Cancer Res 2017;77:996–1007), which appeared in the February 15, 2017, issue of *Cancer Research* (1), the affiliations for Dr. Angelo L. Vescovi were incorrect; Dr. Vescovi's correct affiliations are IRCCS Casa Sollievo della Sofferenza, ISBReMIT- Institute for Stem Cell Biology, Regenerative Medicine and Innovative Therapies, Italy; Department of Biotechnology and Biosciences, University of Milan Bicocca, Milan, Italy; IRCSS Casa Sollievo della Sofferenza, c/o Instituto Mendel, Rome, Italy; and Hyperstem SA, Lugano, Switzerland.

The online version of the article has been corrected and no longer matches the print. The authors regret this error.

Reference

1. Binda E, Visioli A, Giani F, Trivieri N, Palumbo O, Restelli S, et al. Wnt5a drives an invasive phenotype in human glioblastoma stem-like cells. Cancer Res 2017;77:996–1007.

AACR

Cancer Research

AAC-R American Association for Cancer Research

Wnt5a Drives an Invasive Phenotype in Human Glioblastoma Stem-like Cells

Elena Binda, Alberto Visioli, Fabrizio Giani, et al.

Updated version	Access the most recent version of this article at: doi:10.1158/0008-5472.CAN-16-1693
Supplementary Material	Access the most recent supplemental material at: http://cancerres.aacrjournals.org/content/suppl/2016/12/23/0008-5472.CAN-16-1693.DC1

Cited articles	This article cites 49 articles, 9 of which you can access for free at: http://cancerres.aacrjournals.org/content/77/4/996.full#ref-list-1
Citing articles	This article has been cited by 1 HighWire-hosted articles. Access the articles at: http://cancerres.aacrjournals.org/content/77/4/996.full#related-urls

E-mail alerts	Sign up to receive free email-alerts related to this article or journal.
Reprints and Subscriptions	To order reprints of this article or to subscribe to the journal, contact the AACR Publications Department at pubs@aacr.org.
Permissions	To request permission to re-use all or part of this article, use this link http://cancerres.aacrjournals.org/content/77/4/996. Click on "Request Permissions" which will take you to the Copyright Clearance Center's (CCC) Rightslink site.